processes

MDPI

Article

Analysis of Oil Droplet Deposition Characteristics and Determination of Impact State Criterion in Aero-Engine Bearing Chamber

Fei Wang *, Lin Wang * and Guoding Chen

School of Mechanical Engineering, Northwestern Polytechnical University, Xi'an 710072, China; gdchen@nwpu.edu.cn

* Correspondence: wfei@mail.nwpu.edu.cn (F.W.); wanglin@nwpu.edu.cn (L.W.); Tel.: +86-187-2900-1815 (F.W.)

Received: 31 May 2020; Accepted: 24 June 2020; Published: 25 June 2020

Abstract: The research of oil/air two-phase flow and heat transfer is the fundamental work of the design of lubrication and heat transfer in aero-engine bearing chamber. The determination of impact state criterion of the moving oil droplets with the wall and the analysis of oil droplet deposition characteristics are important components. In this paper, the numerical analysis model of the impact between the moving oil droplet and the wall is established by using the finite volume method, and the simulation of oil droplet impingement on the wall is carried out. Then the effects of oil droplet diameter, impact velocity, and incident angle on the characteristic parameters of impact state are discussed. The characteristic parameters include the maximum spreading length, the maximum spreading width, and the number of splashing oil droplets. Lastly the calculation results are verified through comparing with the experimental results in the literature. The results show as follows: (1) The maximum spreading width of oil droplet firstly increases and then slows down with the incident angle and the oil droplet diameter increasing; (2) when the oil droplet diameter becomes small, the influence of the incident angle on the maximum spreading length of oil droplet is obvious and vice versa; (3) with the impact velocity and diameter of oil droplet increasing, the maximum spreading width of oil droplet increases firstly and then slows down, and the maximum spreading length increased gradually; (4) the number of splashing oil droplets increases with the incident angle and impact velocity increasing; and (5) compared with the experimental data in literature, the critical dimensionless splashing coefficient *Kc* proposed in this paper can better distinguish the impact state of oil droplet.

Keywords: aero-engine; bearing chamber; oil droplet; numerical simulation; criterion; splash; deposition; impact; process

1. Introduction

Lubrication oil is supplied to roller or ball bearings via an under-race lubrication method and then sheds into aero-engine bearing chamber in the form of oil droplets. The high-speed moving oil droplets impact with the chamber wall at different incident angles, the diameter of oil droplets is in the range of 1–500 μm, and the impingement time is only a few microseconds. Then the oil droplet or deposits on the wall surface to form oil film, or disintegrates many smaller secondary oil droplets to suspend in the bearing chamber. Thus air, oil droplet, and oil film coexist in the bearing chamber. The whole impingement process can be simplified as the impact of oil droplet with the oblique wall. Meanwhile, the real aero-engine operating conditions are complicated, and the experimental studies are limited. It is very difficult to accurately analyze the air-oil two-phase flow, and restricts the precise design of aero-engine lubrication system. So, the numerical simulation can make up the deficiency

of the experiment method to a large extent. In this paper, the determination of impact state criterion between oil droplet and wall and the analysis of oil droplet disposition characteristics are performed, which can provide more reasonable initial condition for the further research of multiphase flow and heat transfer in the bearing chamber.

The phenomenon of liquid drop impacting with solid wall was firstly observed by Worthin et al. [1] by means of the experiment that water droplet and mercury droplet impact with metal surface. Subsequently, more comprehensive and extensive experimental research had been carried out by many scholars under different parameter conditions. Early research focused on the observation of the droplet shape change after the impact, and the analysis of the influence of droplet physical parameters, impact velocity, and wall roughness. Mundo et al. [2] observed the impact phenomenon of alcohol, water, and solid wall through experimental research, analyzed the influence of physical parameter of solution, impact parameter and droplet diameter on the collision, and introduced the characteristic parameter as the criterion for judging whether the droplet splashes or not. Glahn et al. [3] measured oil droplet sizes and velocities by utilizing a Phase Doppler Particle Analyzer (PDPA) technique for the first time under the real engine conditions, and calculated the droplet trajectories and velocities by using numerical method. Simmons et al. [4] calculated the dispersion oil droplets motions using the two-way coupling method, where the oil droplet diameter is in the range of 1~500 microns. Cossali et al. [5] studied the splashing phenomenon of droplets after impinging on the liquid film by experiments, proposed the definition of splashing, and summarized the critical parameters of splashing. Sikalo et al. [6,7] carried out an experimental study on the impact between the droplet and the inclined wall, found the phenomenon of spread, rebound, and splash appeared after the impact between the droplet and the solid surface, and analyzed the influence of the incident angle and impact velocity of the droplet on the spreading characteristics and rebound rate of the liquid film. Rioboo et al. [8,9] put forward six kinds of impact phenomena between liquid droplet and solid wall based on the observation results of collision test using water and alcohol mixture, and analyzed the influence of the liquid droplet, impact velocity, and the roughness of solid wall on the shape change of splashed liquid droplet and liquid film after collision. Hitoshi and Yu et al. [10] combining experimental and numerical simulation methods, studied the form of spreading water film formed by water droplet after colliding with inclined wall. Shen et al. [11] used a two-dimensional numerical simulation method to compute the dynamic process of water droplet impacting the inclined wall, and analyzed the influence of impact velocity and incident angle of water droplet under the condition of low impact energy on the spreading length. Wang et al. [12] established the collision model of oil droplet and chamber wall based on the motion state before the collision between oil droplet and bearing chamber wall in the aero-engine, and obtained the influence rule of oil droplet diameter on the deposition rate and momentum transfer rate of oil droplet. Fujimoto and Ogino et al. [13] calculated the deformation, velocity, and pressure distribution of liquid droplet when hit the horizontal and inclined surface, and compared them with the experimental results. Fukai et al. [14] used the two-dimensional finite element method to simulate the deformation behavior after the collision of droplet and plates, and analyzed the influence of impacting velocity and contact angle. Lu et al. [15] used the high-speed photography technology to establish the relationship between the spreading characteristics of liquid film, the weber number, and impact incident angle. Vladimir et al. [16] studied the collision of droplet and the oil tank surface by theoretical analysis method, and analyzed the change rule of the adhesion and splashing of a single droplet impact with the oil tank surface. Gorse et al. [17] carried out an experimental study on the oil droplet generation by roller bearing in a wide range of engine conditions, the results revealed that the pressure across the bearing and the structure of the bearing support had strong influence on the generation of oil droplets. Farrall et al. [18] used CFD technique to determine the outcome of droplet impact with a wall film, and the results show that the behavior of oil in bearing chamber is strongly influenced by the conditions with which it leaves the bearing. Chen et al. [19] established the oil droplet movement model in the air fluid by Lagrangian method, and analyzed the deposition characteristics of the moving oil droplet after colliding with the bearing chamber wall. Chen et al. also analyzed the collision between the

deformed oil droplet and the wall, and obtained the change rule of the flow characteristics of the oil film on the wall. Tembely et al. [20] discussed the effect of substrates' wettability on the droplet impact droplet spreading, and the evolution of spreading diameter was determined. Adenyi et al. [21] carried out numerical and experimental study of a customized shallow sump aero-engine bearing chamber with inserts to improve oil residence volume. Bristot et al. [22] identified a Volume of Fluid (VOF) approach with turbulence damping for the transient simulation of air/gas two-phase flows in bearing chamber, which improve the accuracy of bearing chamber flows modelling.

Although there are many researches on the impact between droplet and solid wall, most of them focus on spreading characteristics after the impact between droplet and solid wall. However, the determination of impact state criteria for the adhesion and splashing state of droplet and the variation of the number of secondary droplets after the impact is rarely discussed. Meanwhile, compared with the water droplet, the high viscosity coefficient makes it show inherent characteristics when an oil droplet impacts with the wall. Therefore, it is very necessary to carry out the research on the determination of impact state criteria and the deposition characteristics of moving oil droplets in the bearing chamber.

The VOF method is used to establish the numerical model of oblique collision between moving oil droplet and solid wall. The impact state and the deposition characteristic of oil droplet is calculated under the different oil droplet diameter, incident angle, and impact velocity. Single factor analysis method is employed to analyze oil droplet impact state. The determination of impact state criterion between the dimensionless splashing coefficient and oil droplet impact state is acquired. The results can be applied to the impact analysis of oil droplet and wall in aero-engine bearing chamber. And the quantitative analysis of the number of splashing secondary oil droplets could provide the initial condition for further research on coalescence and breakup of the secondary oil droplet in the bearing chamber.

2. Theory and Calculation Model

2.1. The Governing Equation of Oil Droplet Impacting with the Wall

There are two kinds of fluids involved in the process of impact between oil droplet and the wall: Lubricating oil and air. Both of them are assumed incompressible fluid and no mass and momentum exchanged with each other. The mass and momentum conservation equation of each phase are as follows:

$$\nabla \cdot \boldsymbol{V} = 0 \tag{1}$$

$$\frac{d\boldsymbol{V}}{dt} + \nabla \cdot (\boldsymbol{V}\boldsymbol{V}) = g - \frac{1}{\rho}[\nabla \mathrm{p} - \mu \nabla^2 \boldsymbol{V}] + \frac{1}{\rho}F \tag{2}$$

where $\boldsymbol{V}$ is the fluid velocity; p is the fluid pressure; g is the gravity acceleration; ρ and μ are the average density and average dynamic viscosity of fluid respectively; F is the momentum source term generated by oil surface.

VOF method [23,24] is used to trace the free interface between oil droplet and air, and the volume fraction of oil in grid cell is calculated. The oil volume fraction equation is given by

$$\frac{\partial \Omega}{\partial t} + \boldsymbol{V} \cdot \nabla \Omega = 0 \tag{3}$$

where Ω is the oil volume fraction, $\Omega = 0$ and $\Omega = 1$ indicate that there is no oil or full oil in the grid cell respectively; $0 < \Omega < 1$ indicates that oil and air coexist in the gird cell at the same time.

The average density and dynamic viscosity of the fluid in the grid cell are

$$\rho = \Omega \rho_l + (1 - \Omega)\rho_g \tag{4}$$

$$\mu = \Omega \mu_l + (1 - \Omega)\mu_g \tag{5}$$

where subscript l and g represent oil and air respectively.

According to the continuous surface tension model proposed by Bracketbill et al. [25], the momentum source term in Equation (2) is given by

$$F = \sigma \frac{\rho \kappa \nabla \Omega}{(\rho_l + \rho_g)/2} \tag{6}$$

where κ is the surface curvature, $\kappa = \nabla(\boldsymbol{n}/|n|)$, $\boldsymbol{n}$ is the normal direction of the free interface between oil droplet and air, $\boldsymbol{n} = \nabla\Omega$.

2.2. Numerical Model of Oil Droplet Impacting with Wall

The schematic diagram of the impacting between oil droplet and the solid wall is shown in Figure 1. The diameter of the incident oil droplet is D, the incident angle of the oil droplet is θ, and the impacting velocity is v. The width and length of the wall are W and L respectively.

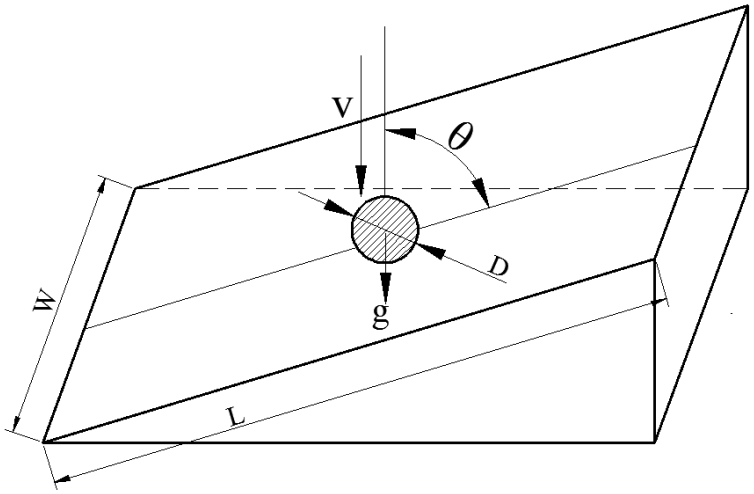

Figure 1. Oil droplet impact with solid wall.

The grid model of oil droplet impacting with solid wall is shown in Figure 2, and the calculation region is W × L × H = 2 mm × 2 mm × 0.4 mm. The boundary conditions of calculation are as follows:

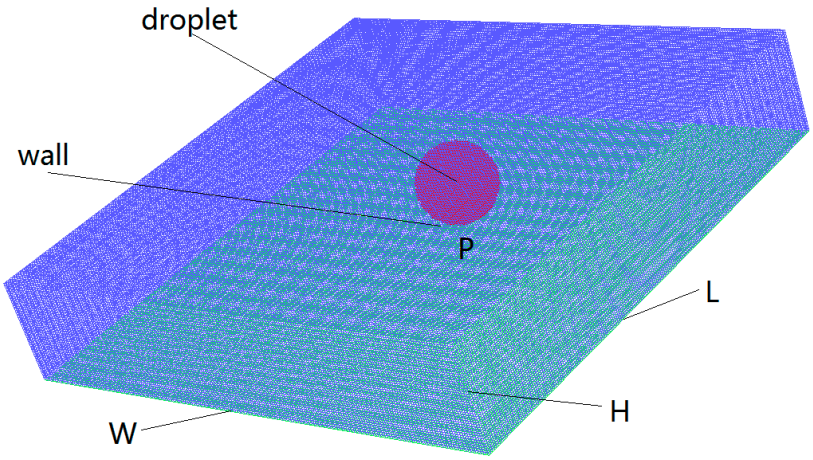

Figure 2. Grid model of moving oil droplet impacting with the wall.

(1) In the calculation area of oil droplet, the volume fraction of oil is set as 1, the initial oil droplet velocity is the impacting velocity;

(2) in the other calculation area, the volume fraction of oil is set as 0; and
(3) the wall adopts the no-slip velocity boundary condition.

The impact point of oil droplet and the wall is P. Hexahedral structured grids are generated in the entire computational domain. In order to ensure the calculation accuracy, W and L are divided into 200 segments respectively, and H is divided into 40 segments. The volume cell is 1 μm × 1 μm × 1 μm, and the total grid number is 1,600,000. The mesh quality is quite fine, which completely meets the computing requirement. Considering the accuracy and sharpness, the Geo-Reconstruct is employed for interface reconstruction. And the second-order upwind scheme is employed for discretization of fluid mass and momentum conservation equation. The transient solver is used to solve the equations, in which Presto algorithm is employed for the pressure term, PISO algorithm is used for coupling the pressure and velocity term: where oil density ρ_l is 926 kg/m^3, dynamic viscosity μ_l is 0.007 P·s, and surface tension coefficient σ_l is 0.035 N/m. Gas density ρ_g is 1.225 kg/ m^3, dynamic viscosity μ_g is 1.789×10^{-5} P·s.

3. Results and Discussion

In this paper, the deposition characteristics of oil droplet are calculated under different operating condition. The impacting velocity, incident angle and oil droplet diameter chosen are derived from the literature [3,12,19]. The specific parameters and values are shown in Table 1.

Table 1. Operating condition.

Parameters	Value
Impacting velocity v (m/s)	10,15,20,25,30
Incident angle θ (°)	30,45,60,75
Oil droplet diameter D (μm)	100,150,200,250,300

3.1. Deposition Characteristics of Oil Droplet under Different Oil Droplet Diameter, Velocity, and Incident Angle

The adhesion and spreading process of oil droplet in 60 μs is shown in Figure 3 when the diameter is 150 μm, the impacting velocity is 15 m/s and the incident angle is 30°. The adhesion and spread indicates that there are no secondary oil droplets appeared after the oil droplet impacting the wall. After impacting with the solid wall, the oil droplet spread along the wall under the combined action of gravity, inertial force, surface tension, and viscous force. It can be seen from the figure that the spreading length and spreading width of the oil film are quite different, and the oil film distribution is asymmetrical in the direction W and L. The oscillation and accumulation phenomenon occurred at the bottom of the oil film, accompanied by the appearance of "dry out spots". The reason is that the force of oil droplet is uneven in the direction of spreading length and width. Due to that the incident angle is small, the effect of gravity and viscous force on the direction of spreading length are more significant, but the spread in the direction of width is only affected by viscous force.

The adhesion and spreading process of oil droplet in 60 μs is shown in Figure 4 when the diameter is 200 μm, the impacting velocity is 10 m/s and the incident angle is 60°. Compared with Figure 3, the spread of oil droplet on the wall is quite different. Under this condition, the spread shape of oil droplet on the wall is approximately circular, and the spread is relatively uniform in the direction of length and width. The reason is that the effect of gravity on the oil droplet become small with the incident angle increasing, and surface tension and viscous force plays a leading role.

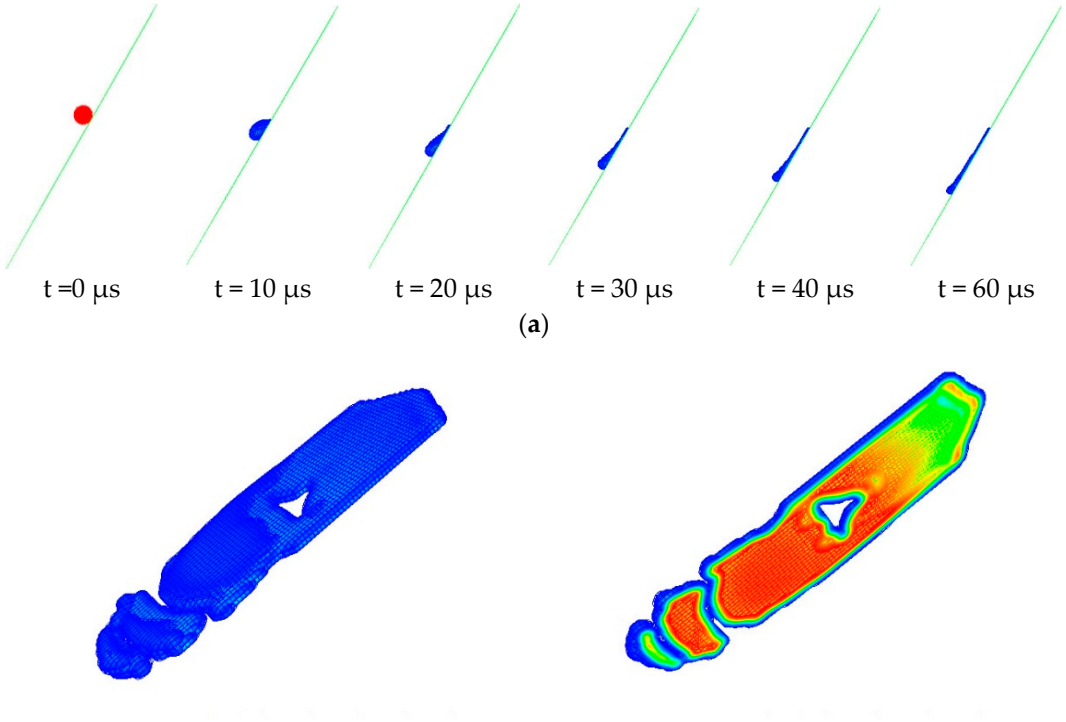

Figure 3. Spreading process of oil droplet (D = 150 μm, v = 15 m/s, θ = 30°), where the contour plots represent the volume fraction of oil droplet. (**a**) Spreading process of oil droplet in 60 μs. (**b**) Spreading of oil droplet at 60 μs.

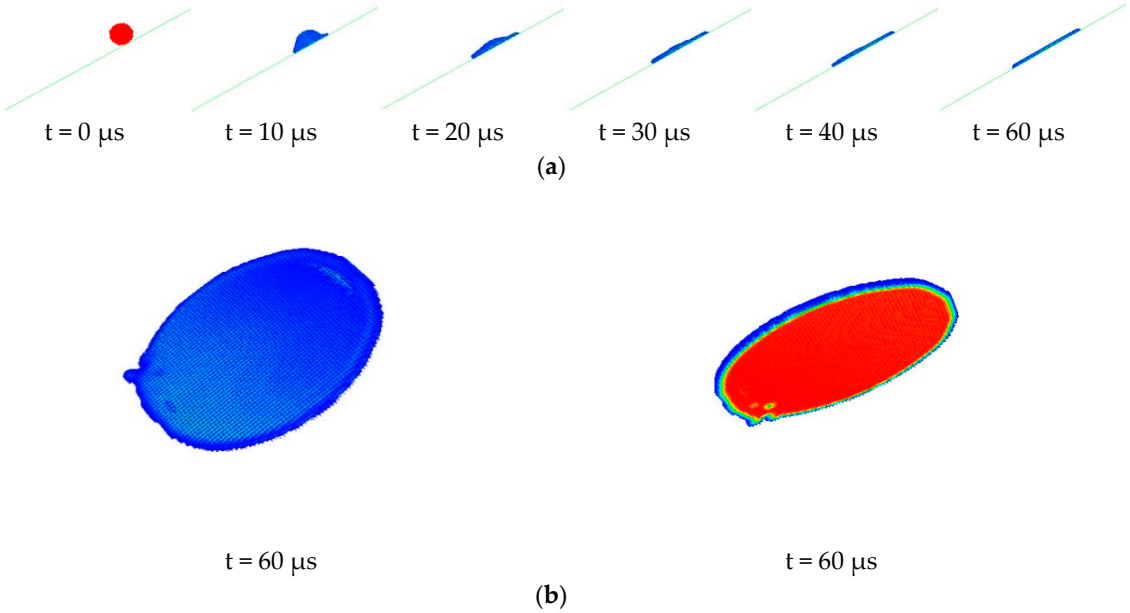

Figure 4. Spreading process of oil droplet (D = 200 μm, v = 10 m/s, θ = 60°), where the contour plots represent the volume fraction of oil droplet. (**a**) Spreading process of oil droplet in 60 μs. (**b**) Spreading of oil droplet at 60 μs.

The adhesion and spreading process of oil droplet in 60 μs is shown in Figure 5 when the diameter is 250 μm, the impacting velocity is 25 m/s and the incident angle is 60°. It can be seen that the oil

droplet splashed after impacting with the wall. Due to that the diameter of the oil droplet is large and the impacting velocity is high, so the momentum of the impacting oil droplet is larger. But a large incident angle reduced the flow velocity of the deposited oil film along the wall, and the propagation velocity of the internal shock wave of the oil film is faster than that of the oil film along the wall, so "small oil column" appears at the edge of the spreading oil film. With the aid of the propagation of the shock wave, the energy accumulated at the edge, and "small oil column" extends upward, thus the "small oil column" breaks up and forms the second small splashing oil droplet. Meanwhile, it can be seen that the oil film also breaks up under the action of shock wave, which results in uneven spreading thickness of oil film on the wall, and accompanies by the appearance of dry out spots.

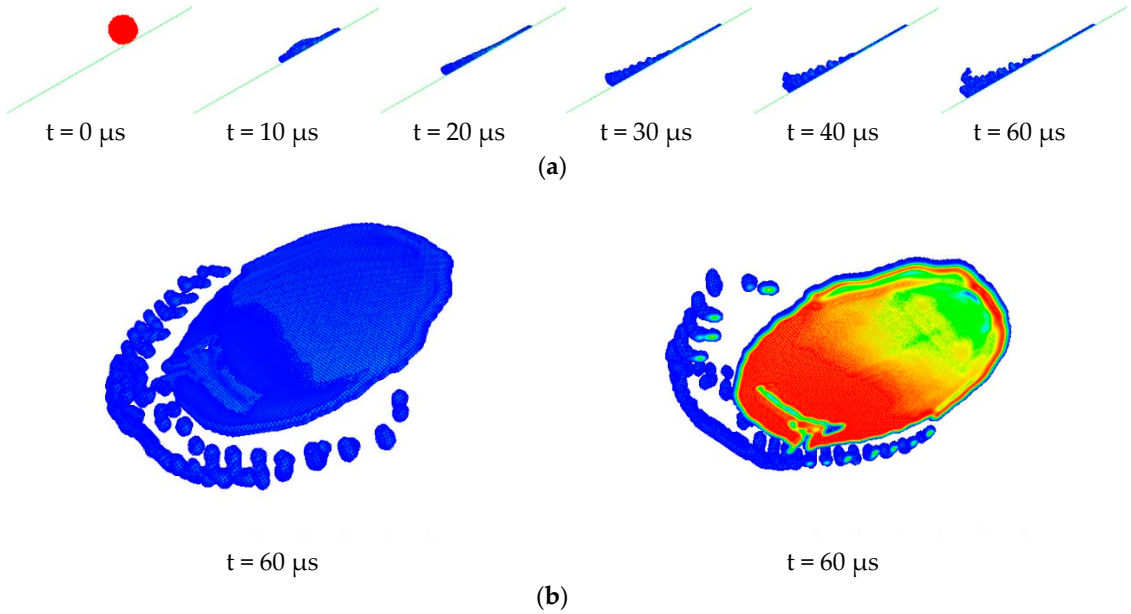

Figure 5. Splashing process of oil droplet (D = 250 μm, v = 25 m/s, θ = 60°), where the contour plots represent the volume fraction of oil droplet. (**a**) Splashing process of oil droplet in 60 μs. (**b**) Splashing of oil droplet at 60 μs.

The characteristic parameters include the maximum spreading length, the maximum spreading width, and the number of splashed secondary oil droplet, which are used to characterize the change rule of the impact state between the oil droplet and the solid wall. Figure 6 shows the relationship of the maximum spreading length and the maximum spreading width of the deposited oil film with the diameter of oil droplet under different incident angles when the impacting velocity is 20 m/s. The maximum spreading width of the oil film increases with the diameter and incident angle of oil droplet increasing, and the spreading width of the oil film increases firstly and then gradually slows down. With the diameter and incident angle of oil droplet increasing, the splash phenomenon occurs after the oil droplet impacting with the wall. The relationship between the maximum spreading length of the oil film, the diameter and the incident angle of the oil droplet is complicated. When the incident angle is small, the oil droplet is significantly affected by gravity. So, the maximum spreading length of the oil film is large. However, with the diameter of oil droplet increasing, the influence of incident angle on maximum spreading length of oil film weakens.

In Figure 7, the relationship of the maximum spreading length and width of deposited oil film with the diameter of impacting oil droplet under different impacting velocity when the incident angle is 60° and the spreading time is 60 μs. It can be seen that with the impacting velocity increasing, the maximum spreading width of oil film increases firstly and then slows down, while the maximum spreading width of oil film increases with the impacting velocity and oil droplet diameter increasing. The larger impacting velocity and kinetic energy of oil droplet, the greater remaining energy after the

oil droplet overcomes the energy dissipation in the spreading process, which is conducive to the further spreading. However, due to the splashing phenomenon on the edge of spreading, the spreading width slows down.

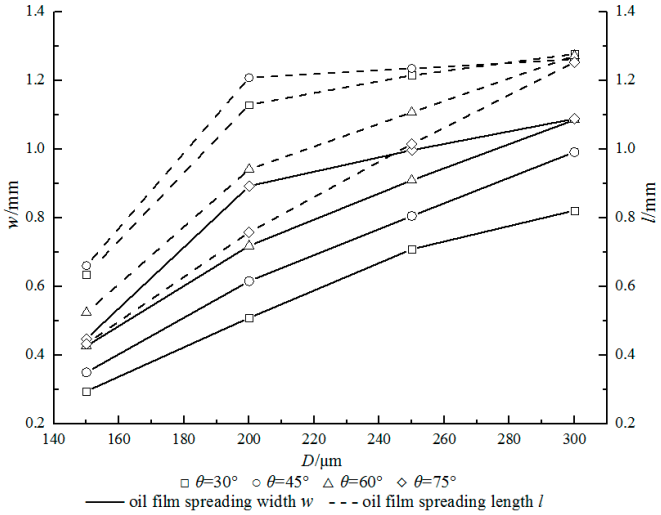

Figure 6. Effect of incident angle on spreading characteristics of deposited oil film when the impacting velocity is 20 m/s.

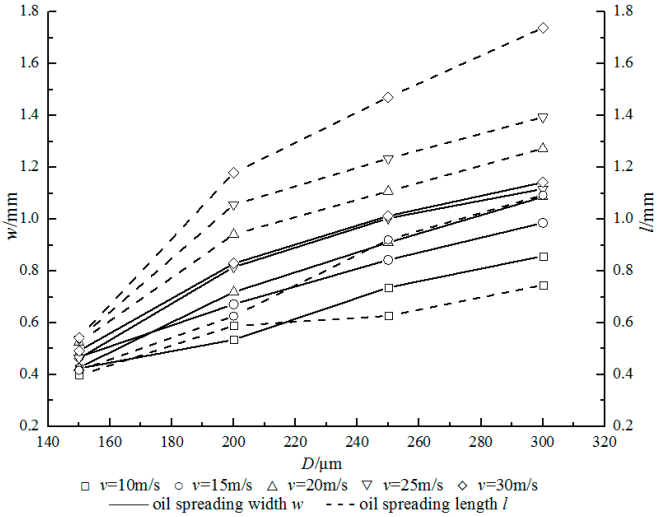

Figure 7. Effect of impacting velocity on spreading characteristics of deposited oil film when the incident angle is 60°.

The trend of oil droplet impacting velocity and the number of splashed oil droplet under different incident angles is shown in Figure 8 when the oil droplet diameter is 300 μm and the spreading time is 60 μs. It can be seen that when the impacting velocity of oil droplet is low, no splash occurs after the impact between oil droplet and the wall. With the impacting velocity of oil droplet increasing, the number of splashed oil droplet increases. Obviously, the reason is that the higher impacting momentum of oil droplet with larger impacting velocity, the more splashing oil droplet produced. Meanwhile, with the incident angle increasing, more splashing oil droplets are born at the same impacting velocity. The oil film is more evenly stressed in the length and width direction with the incident angle increasing. And more small oil columns emerge at the edge of the oil film, then occurs fracture, so more splashing oil droplets are produced.

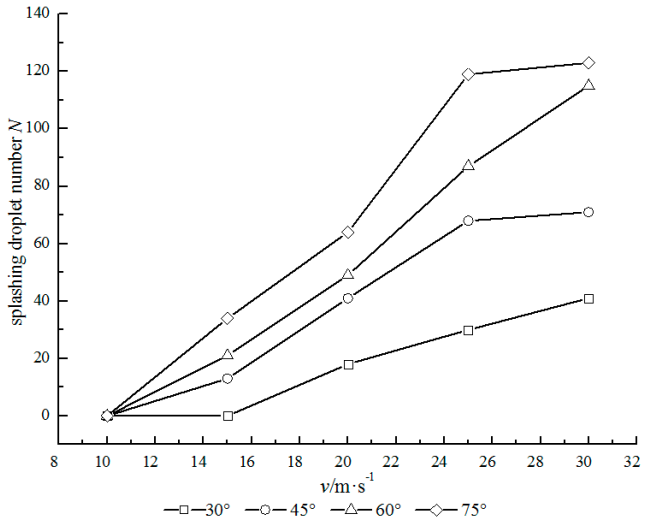

Figure 8. Effect of impact velocity on the number of splashed oil droplets when the oil droplet diameter is 300 μm.

3.2. Determination of Impact State Criterion

The determination of impact state criterion of moving oil droplet and the wall indicates that the criterion can judge whether the critical state of oil droplet splashing occurred after the impacting with the wall. According to the previous analysis, whether the splashing phenomenon occurs is depended on the geometric and motion parameters such as the diameter, impacting velocity and incident angle of oil droplet. The relevant parameters are derived from the literature [9,14]. In order to determine whether the splashing phenomenon occurred after oil droplet impacted with the wall in the bearing chamber, the single factor analysis method is employed in a wide range of parameter. The numerical simulation of impact state between oil droplet and the wall are carried out to compute the deposition and splashing of oil droplet under the combination of several influence parameters. The value of the combination of geometric and motion parameter are recorded under corresponding conditions. In order to establish the criterion for judge the critical state of moving oil droplet impacting the wall, the dimensionless splashing coefficient K is introduced, and the expression is given by

$$K = We^{0.5} Re^{0.25} \tag{7}$$

where

$$We = \rho_l v^2 D / \sigma_l \tag{8}$$

$$Re = \rho_l v D / \mu_l \tag{9}$$

where ρ_l is oil droplet density; v is oil droplet impacting velocity; D is oil droplet dimeter; σ_l is surface tension of oil droplet; μ_l is dynamic viscosity of oil droplet. We is the Weber number. Re is Reynolds number.

The distribution relationship between the combination of geometric and operating parameters and the dimensionless splashing coefficient K which correspond to the oil droplet deposition and splashing state is shown in Figure 9. In the figure, the deposition and splashing of oil droplet are divided into two parts. The dimensionless splashing coefficient corresponding to the fitted curve was known as critical dimensionless splashing coefficient, which was represented by Kc. The fitting relationship between the dimensionless splashing coefficient and the incident angle of oil droplet obtained by univariate nonlinear regression analysis, which is given by

$$Kc = 182.657 \times \theta^{-0.5543} \tag{10}$$

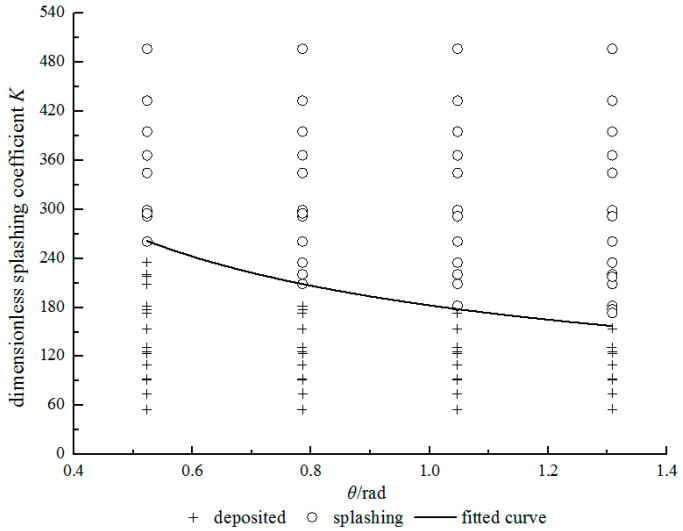

Figure 9. Distribution relationship between oil droplet deposition or splashing state and dimensionless splashing coefficient *K*.

The significance of the critical dimensionless splashing coefficient is that: (1) when $K < Kc$, the moving oil droplet will deposit after impacting with the solid wall, and no secondary oil droplet will be produced; (2) when $K > Kc$, the moving oil droplet will splash after impacting with the wall, and secondary oil droplet will be produced. The critical dimensionless splashing coefficient can be used as a criterion to judge the impact state between the oil droplet and the wall in the aero-engine bearing chamber.

3.3. Verification and Comparison of Impact State between Oil Droplet and the Wall

The dimensionless splashing coefficient can be used as the judgment criterion for the impact state of moving oil droplet and solid wall. In order to verify the rationality and validity, the critical dimensionless splashing coefficient and the judgment results provided in this paper are compared with the relevant experimental results in the literature [2,6,26], as shown in Table 2. Through comparison, it is found that the results of this paper are consistent with experimental results in the literature, and the critical dimensionless splashing coefficient proposed in this paper can better distinguish the impact state of oil droplet. The criterion for determining the impact state between moving oil droplet and the wall can be applied to the aero-engine bearing chamber, which has not been achieved in the existing research work.

Table 2. Comparison with the experimental results.

D (mm)	ρ_l (kg/m^3)	μ_l (Pa·s)	σ_l (N/m)	θ (°)	v (m/s)	Experimental Results of [2,6,26]	Dimensionless Splashing Coefficient K of This Paper	Judgement Results of This Paper
0.132	786	0.0024	0.021	54°	17	splashing [2]	196.74	splashing
0.5	1000	0.000894	0.072	90°	18.81	splashing [26]	502.02	splashing
0.5	1000	0.000894	0.072	90°	32.54	splashing [26]	995.98	splashing
0.5	1000	0.0021	0.069	90°	18.27	splashing [26]	399.41	splashing
0.5	1050	0.0021	0.069	90°	32.92	splashing [26]	864.90	splashing
0.5	684	0.000387	0.020	90°	14.23	splashing [26]	623.14	splashing
0.5	684	0.000387	0.020	90°	8.93	splashing [26]	348.05	splashing
0.5	714	0.000720	0.022	90°	7.56	splashing [26]	238.29	splashing
0.5	714	0.000720	0.022	90°	13.28	splashing [26]	481.90	splashing
2.45	1220	0.116	0.063	90°	1.04	deposited [6]	16.30	deposited
2.72	996	0.001	0.072	10°	3.25	deposited [6]	193.119	deposited
2.72	996	0.001	0.072	45°	3.25	splashing [6]	193.11	splashing
2.72	996	0.001	0.072	45°	1.55	deposited [6]	76.54	deposited
3.3	786	0.0024	0.021	45°	2.1	splashing [6]	161.08	splashing

4. Conclusions

(1) The influence of incident angle on the maximum spreading length of oil droplet is large when the diameter of oil droplet is small; the influence of incident angle on the maximum spreading length of oil droplet is small when the diameter of the oil droplet is large; while the maximum spreading width of the oil droplet increases firstly and then slows down with the incident angle increasing.

(2) With the oil droplet diameter and impacting velocity increasing, the maximum spreading width increasing firstly and then slows down, while the maximum spreading length shows an increasing trend.

(3) With impacting velocity and incident increases, the number of splashing oil droplet presents an increasing trend under the condition of splashing caused by oil droplet impacting with the wall.

(4) Compared with the physical experiments in the literature, the rationality and validity of the critical dimensionless splashing coefficient proposed in this paper is verified. It is shown that the dimensionless splashing coefficient is feasible as a criterion for judging the impact between the moving oil droplet and the solid wall in the bearing chamber.

Author Contributions: Conceptualization, F.W.; Methodology, F.W.; Software, F.W; Validation, F.W.; Formal Analysis, F.W. Investigation, F.W. and L.W. Writing-original draft preparation, F.W.; Writing—Review and Editing, F.W., L.W., G.C.; Supervision, G.C.; Project Administration, G.C.; Funding Acquisition, L.W. All authors have read and agreed to the published version of the manuscript.

Funding: This research was funded by the National Natural Science Foundation of China, grant number 51975475.

Conflicts of Interest: The authors declare no conflicts of interest.

Nomenclature

ρ	average density of fluid
μ	average dynamic viscosity of fluid
ρ_l	oil density
ρ_g	gas density
μ_l	oil dynamic viscosity
σ_l	oil surface tension coefficient
μ_g	air dynamic viscosity
θ	incident angle of oil droplet
κ	surface curvature
Ω	oil volume fraction
p	fluid pressure
D	diameter of oil droplet
F	momentum source term generated by oil surface
g	gravity acceleration
$\boldsymbol{n}$	normal direction of the free interface between oil droplet and air
v	impacting velocity of oil droplet
We	Weber number
Re	Reynolds number
K	dimensionless splashing coefficient
Kc	Critical dimensionless splashing coefficient

References

1. Worthington, A.M. On the forms assumed by drops of liquids falling vertically on a horizontal plate. *Proc. R. Soc. Lond.* **1876**, *25*, 171–178.
2. Mundo, C.; Sommerfeld, M.; Tropea, C. Droplet wall collisions: Experimental studies of the deformation and breakup process. *Int. J. Multiph. Flow* **1995**, *21*, 151–173. [CrossRef]

3. Glahn, A.; Kurreck, M.; Willmann, M.; Wittig, S. Feasibility study on oil droplet flow investigations inside aero engine bearing chambers—PDPA techniques in combination with numerical approaches. *J. Eng. Gas Turbines Power* **1996**, *118*, 749–755. [CrossRef]
4. Simmons, K.; Hibberd, S.; Wang, Y.; Care, I. Numerical study of the two-phase air/oil flow within an aero-engine bearing chamber model using a coupled Lagrangian droplet tracking method. In Proceedings of the ASME Pressure Vessels and Piping Conference, Vancouver, BC, Canada, 5–9 August 2002.
5. Cossali, G.E.; Coghe, A.; Marengo, M. The impact of a single drop on a wetted solid surface. *Exp. Fluids* **1997**, *22*, 463–473. [CrossRef]
6. Sikalo, S.; Tropea, C.; Ganic, E.N. Impact of droplets onto inclined surfaces. *J. Colloid Interface Sci.* **2005**, *286*, 661–669. [CrossRef]
7. Sikalo, S.; Ganic, E.N. Phenomena of droplet surface interactions. *Exp. Therm. Fluid Sci.* **2006**, *31*, 97–110. [CrossRef]
8. Rioboo, R.; Tropea, C.; Marengo, M. Outcomes from a drop impact on solid surfaces. *At. Sprays* **2001**, *11*, 155–165. [CrossRef]
9. Rioboo, R.; Marengo, M.; Tropea, C. Time evaluation of liquid drop impact onto solid dry surfaces. *Exp. Fluids* **2002**, *33*, 112–121. [CrossRef]
10. Hitoshi, F.; Yu, S. Three-dimensional numerical analysis of the deformation behavior of droplets impinging onto a solid substrate. *Int. J. Multiph. Flow* **2007**, *33*, 317–332.
11. Shen, S.Q.; Cui, Y.Y.; Guo, Y.L. Numerical simulation of droplet striking on inclined isothermal surface. *J. Therm. Sci. Technol.* **2009**, *8*, 194–197. (In Chinese)
12. Wang, J.; Chen, G.D.; Liu, Y.J. Analysis of the oil droplet motion and deposition Characteristics in an aeroengine bearing chamber. *Tribology* **2010**, *30*, 362–366. (In Chinese)
13. Fujimoto, H.; Ogino, T. Collision of a droplet with a hemispherical static droplet on a solid. *Int. J. Multiph. Flow* **2001**, *27*, 1227–1245. [CrossRef]
14. Fukai, J.; Tanaka, M.; Miyatake, O. Maximum spreading of liquid droplets upon impact on flat surface. *J. Chem. Eng. Jpn.* **1998**, *31*, 456–461. [CrossRef]
15. Lu, J.; Chen, X.L.; Cao, X.K. Characteristic phenomenon and analysis of a single liquid droplet impacting on a dry surface. *Chem. React. Eng. Technol.* **2007**, *12*, 505–511. (In Chinese)
16. Weinstock, V.D.; Heister, S.D. Modeling oil flows in engine sumps: Drop dynamics and wall impact simulation. *J. Eng. Gas Turbines Power Trans. ASME* **2006**, *128*, 163–172. [CrossRef]
17. Gorse, P.; Dullenkopf, K.; Bauer, H.-J.; Wittig, S. An Experimental Study on Droplet Generation in Bearing Chambers Caused by Roller Bearings. In Proceedings of the ASME Turbo Expo 2008: Power for Land, Sea, and Air, Berlin, Germany, 9–13 June 2008.
18. Farrall, M.; Simmons, S.; Hibberd, S.; Gorse, P. Modeling Oil Droplet/Film Interaction in an Aero-Engine Bearing Chamber and Comparison with Experimental Data. ASME Paper No. GT2004–53698. In Proceedings of the ASME Turbo Expo 2004: Power for Land, Sea, and Air, Vienna, Austria, 14–17 June 2004.
19. Chen, B.; Chen, G.D.; Wang, T. Flow characteristics analysis of wall oil film with consideration of oil droplet deformation and secondary oil droplet deposition in aeroengine bearing chamber. *Acta Aeronaut. Astronaut. Sin.* **2013**, *34*, 1980–1989.
20. Tembely, M.; Vadillo, D.; Soucemarianadin, A.; Dolatabadi, A. Numerical Simulations of Polymer Solution Droplet Impact on Surfaces of Different Wettabilities. *Processes* **2019**, *7*, 798. [CrossRef]
21. Adeniyi, A.A.; Morvan, H.P.; Simmons, K.A. A Transient CFD Simulation of the Flow in a Test Rig of an Aeroengine Bearing Chamber. In Proceedings of the ASME Turbo Expo2014: Turbine Technical Conference and Exposition, Düsseldorf, Germany, 16–20 June 2014.
22. Bristot, A.; Morvan, H.; Simmons, K. Evaluation of a volume of fluid CFD methodology for the oil film thickness estimation in an aero-engine bearing chamber. In Proceedings of the ASME Turbo Expo 2016: Turbomachinery Technical Conference and Exposition, Seoul, Korea, 13–17 June 2016.
23. Hirt, C.W.; Nichols, B.D. Volume of fluid (VOF) method for the dynamics of free boundaries. *J. Comput. Phys.* **1981**, *39*, 201–225. [CrossRef]
24. Youngs, D.L. Time dependent multi-material flow with large fluid distortion. In *Numerical Methods for Fluid Dynamics*; Morton, K.W., Baines M.J., Eds.; Academic Press: New York, NY, USA, 1982; pp. 273–285.

25. Brackbill, J.U.; Kothe, D.B.; Zemach, C. A continuum method for modeling surface-tension. *J. Comput. Phys.* **1992**, *100*, 335–354. [CrossRef]
26. Pan, K.L.; Tseng, K.C.; Wang, C.H. Breakup of a droplet at high velocity impacting a solid surface. *Exp. Fluids* **2010**, *48*, 143–156. [CrossRef]